Heat Transfer from Moving Fibers in Melt Spinning Process

B. T. F. CHUNG* and V. IYER

Department of Mechanical Engineering, University of Akron, Akron, Ohio 44325

SYNOPSIS

The purpose of this study is to develop a steady-state thermal model for melt spinning of polyester fiber by incorporating the radial heat conduction inside the fiber and the combined effect of radiation and convection at the boundary. The governing equations are obtained from the energy, mass, and momentum balances coupling with the rheological properties of the fibers. The effects of drag, surface tension, gravity, and inertia force are also taken into consideration in the analysis. The velocity profile, temperature profile, and the variation of cross-sectional area of the filament along the axial direction are solved by employing a finite-difference scheme.

INTRODUCTION

In melt spinning the molten polymer is extruded from the spinneret orifice into the cross-flow air, whose temperature is below the solidification point of the polymer. Between the spinneret hole and the take-up device (see Fig. 1) the molten polymer is deformed, cooled, solidified, and transformed into fiber. The fiber formation involves irreversible change of many structural and macroscopic characteristics of the material.

The transition from the molten polymer to the fiber is associated with the change of temperature, composition, and the molecular structure depending on different spinning parameters. Ziabicki[1] points out that the average temperature gradient in melt spinning is in the order of 10^3–10^4 °C/cm. The small difference of 2–3°C between the surface and the core brings about a large tensile viscosity difference in the range of 10–40%. This percent viscosity difference causes the surface of the fiber to solidify while its core is still fluid. The tensile viscosity depends on polymer type, intrinsic viscosity, temperature, rate of deformation, etc., but in this study an Arrhenius type of temperature dependence is used. The large difference viscosity along with the tensile stress brings about a large variation of radial structure in the fiber. These facts illustrate the importance of radial temperature gradient on the internal structure of the fiber. In the extrusion of molten polymers the temperature lies in the range of 500–600 K. At this temperature level the effect of radiation can be appreciable.

Due to its importance in polymer processing, the topic on heat transfer from polyester fibers has been subjected to extensive study in the past decades. Barnett[2] used an empirical correlation and evaluated the temperature distribution inside the fiber, when the fiber moves steadily in a quiescent atmosphere. However, a constant cross-sectional area of the polyester fiber was assumed throughout the analysis. Copley and Chamberlain[3] experimentally found that in melt spinning the filament attenuates exponentially toward its final diameter while moving in an inert atmosphere. Moutsoglou and Bhattacharya[4] improved upon the analysis made by Barnett[2] and Copley and Chamberlain,[3] but the fiber was modeled in a quiescent atmosphere. Morrison[5] predicted the temperature profile of the filament undergoing the solidification process. His model was overly simplified because the rheological properties of the polymer were neglected. Kase and Matsuo[6] and Kase[7] introduced a set of differential equations simulating the fiber being melt spun. Both radial heat conduction and radiation at the boundary were neglected.

In melt spinning process, fiber structures are highly dependent on the rheological characteristics and radial temperature gradient, so it becomes pertinent to reexamine the dynamics of melt spinning. Furthermore, because of the small cross-sectional

* To whom correspondence should be addressed.

Journal of Applied Polymer Science, Vol. 44, 663–670 (1992)
 CCC 0021-8995/92/040663-08$04.00

area of the fiber, there does not exist any experimental method to evaluate the temperature gradient across the cross section of the fiber. Therefore the radial temperature gradient has to be estimated from the theoretical analysis. In the present study an attempt is made to develop a comprehensive mathematical model of the melt spinning of the polyester fiber by incorporating the radial heat conduction in the fiber and the combined radiation and convection at the boundary. The governing equations are formulated from the energy, mass, and momentum balances. To make the analysis complete, the effects of drag, inertia, surface tension, and gravity are also incorporated.

Essentially the present study attempts to extend the earlier work of Kase and Matsuo[6] by including internal thermal resistance of the fiber and external radiative effect at the steady state.

Analysis

In formulation of the governing equations for melt spinning the following simplifying assumptions are made:

1. Die swell is neglected.
2. The cross-sectional area of the fiber is circular.
3. The thermal properties of the fiber such as density, thermal conductivity, and specific heat are constant.
4. The aerodynamic and thermal interaction between neighboring fibers is neglected.
5. The tensile viscosity is assumed to be a function of temperature only.
6. Steady state holds.
7. The spinline is vertical.
8. Heat of crystalization is negligible.

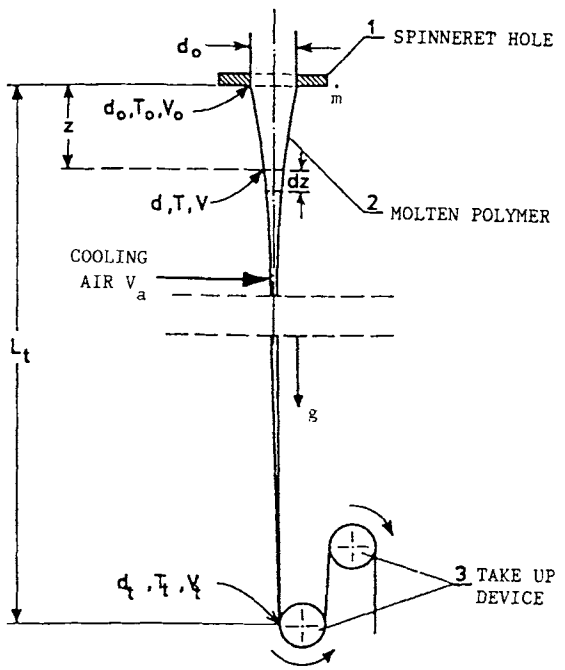

Figure 1 Schematic of polymer processing.

These assumptions, except for 1 and 5, are found to be valid in industrial spinning conditions and incorporate certain limitations on the model. The effects of temperature-dependent properties ρ and C_p have been treated by Nakamura, Katayama, and Amano[8] and are found to be small.

Consideration is given to the schematic diagram shown in Figure 1. Melt spinning is extruded at constant temperature T_0, with a mass flow rate $\dot{m}$, through a spinneret hole with diameter d_0. The constant $\dot{m}$ and ρ determine the velocity at the spinneret hole, v_0. The take-up device is mounted at a distance L_t from the spinneret hole. The solidified polymer is taken up at a velocity v_t and the diameter of spun fiber is d_t. The spinning of fiber is performed in a gaseous medium where the velocity of cross cooling air is v_a.

Applying the conservation of mass, momentum, and energy of the differential element of molten polymer, dz along with the application of rheological properties of polymers, we obtain the following expressions:

$$\frac{d(Av)}{dz} = 0 \tag{1}$$

$$\rho A\left(v\frac{dv}{dz}\right) = \frac{dF}{dz} + \frac{d}{dz}(S_T\sqrt{\pi A}) + \rho gA - 2D_f\sqrt{\pi A} \tag{2}$$

$$v\frac{\partial T}{\partial z} = a\left(\frac{1}{r}\frac{\partial}{\partial r}r\frac{\partial T}{\partial r}\right) \tag{3}$$

$$\frac{dv}{dz} = \frac{F}{\beta A} \tag{4}$$

Details of derivation of Eqs. (1)-(3) are presented by Iyer.[9] In the preceding expressions, F, S_T, D_f, and a are tensile force, surface tension, drag force, and thermal diffusivity, respectively. In Eq. (4) β is the tensile viscosity. In this study, as mentioned earlier, β has an Arrhenius type of temperature dependence, plus an abrupt solidification at

temperature T_s, which was set equal to 60°C following Kase and Matsuo.[6]

$$\beta = \beta_\infty \exp\left(\frac{E}{T + 273}\right) \qquad T \geq T_s$$
$$= \infty \qquad T < T_s \tag{5}$$

where E is the activation energy of the polymer and β_∞ is the material parameter for the polymer used. In spite of simplicity, this tensile viscosity model has produced good simulation results under industrial spinning conditions, probably because the effects of temperature are far stronger than viscoelasticity; consequently making use of more complex rheological models is not mandatory as demonstrated by Kase.[7]

The first term on the right-hand side of Eq. (2) represents the tensile force contribution, the second term relates to the surface tension, the third term is due to gravity, and the last term is associated with the drag force.

The boundary conditions for Eqs. (1)–(4) are

$$T = T_0 \quad v = v_0 \quad A = A_0 \quad d = d_0 \quad r = R_0 \qquad \text{at } z = 0$$

$$T = T_t = T_s \quad v = v_t \quad \text{at } z = L$$

$$\frac{\partial T}{\partial r} = 0 \quad \text{at } r = 0$$

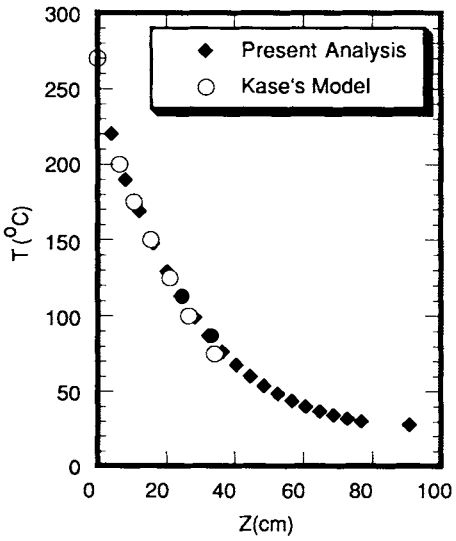

Figure 2 Comparison of the present limiting solution with kase's model.

Table I Range of Parameters

Parameters	Minimum	Maximum
Nondimensional parameter, K	7.0	20.0
Thermal conductivity, cal/cm² sec °C	3.3×10^{-4}	10^{-3}
Spinneret temperature, T_0°C	230.0	270.0
Cross-flow velocity, V_∞ cm/s	5.0	50.0
Ambient temperature, T_∞°C	10.0	40.0
Coefficient of inertia, A_1	0.0	0.4
Coefficient of drag, A_2	0.0	2.5
Coefficient of gravity, A_3	0.0	40.0
Coefficient of surface tension, A_4	0.0	10.0

$$-k\frac{\partial T}{\partial r} = h(T - T_\infty) + \sigma\epsilon(T^4 - T_\infty^4) \qquad \text{at } r = r_b \tag{6}$$

where σ is the Stefan–Boltmann constant, ϵ is emissivity, and r_b is the radius of the fiber.

The experimental correlations developed by Kase and Matsuo[6] for the heat transfer coefficient and for air drag force acting on the spin line are used in the present analysis. They are

$$h = 0.473 \times 10^{-4} A^{-0.333} v^{0.334}\left[1 + \left(\frac{8v_a}{v}\right)^2\right]^{0.167} \tag{7}$$

$$2D_f\sqrt{\pi A} = 3.122 \times 10^{-4} A^{0.095} v^{1.19} \tag{8}$$

where v_a is the velocity of the cross-flow air.

Substituting Eq. (8) into Eq. (2) yields

$$\rho A\left(v\frac{dv}{dz}\right) = \frac{dF}{dz} + \frac{d}{dz}(S_T\sqrt{\pi A}) + \rho g A - 3.122 \times 10^{-4} A^{0.095} v^{1.19} \tag{9}$$

The governing equations are first transformed into dimensionless forms with the aid of the following dimensionless parameters:

$$Z = \frac{z}{L_t} \quad R = \frac{r}{R_0} \quad V = \frac{v}{v_0} \quad \Phi = \frac{A}{A_0}$$

$$V_a = \frac{v_a}{v_0} \quad \theta = \frac{T}{T_0} \quad \theta_\infty = \frac{T_\infty}{T_0}$$

$$\eta = FL_t\left\{A_0 v_0 \beta_\infty \exp\left(\frac{E}{T_0 + 273}\right)\right\}^{-1} \tag{10}$$

Note that all temperatures T, T_0, and T_∞ are expressed in degree Centigrade.

By introducing Eq. (10) into Eqs. (1), (3)–(6), and (9) the following dimensionless governing equations are obtained:

$$\frac{d(\Phi V)}{dZ} = 0 \tag{11}$$

$$\frac{d\eta}{dZ} = A_1\Phi\left(V\frac{dV}{dZ}\right) + A_2\Phi^{0.095}V^{1.19} - A_3\Phi - A_4\frac{d\sqrt{\Phi}}{dZ} \tag{12}$$

$$\Phi\frac{dV}{dZ} = \frac{\eta\exp\left(\dfrac{E}{T_0 + 273}\right)}{\exp\left(\dfrac{E}{T_0\theta + 273}\right)} \tag{13}$$

$$V\frac{\partial\theta}{\partial Z} = \frac{K}{R}\left(\frac{\partial}{\partial R}R\frac{\partial\theta}{\partial R}\right) \tag{14}$$

The associated boundary conditions are

$$R = V = \theta = \Phi = 1.0 \quad \text{at } Z = 0 \tag{15}$$

$$V = V_t \quad \theta = \theta_t \quad \text{at } Z = L/L_t \tag{16}$$

$$\frac{\partial\theta}{\partial R} = 0 \quad \text{at } R = 0 \tag{17}$$

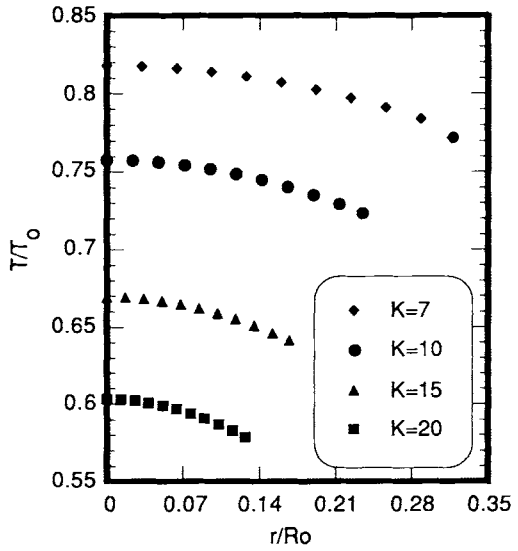

Figure 3 Radial temperature profile, $R_0 = 0.02$ cm, $T_0 = 270°C$, $z/L_t = 0.1436$ cm.

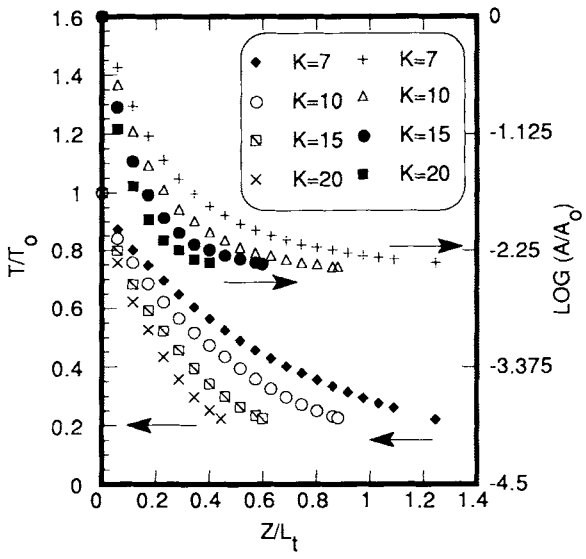

Figure 4 Area and temperature profiles for various values of K, $L_t = 100$ cm, $R_0 = 0.02$ cm, $T_0 = 270°C$.

$$-\frac{\partial\theta}{\partial R} = \frac{hr_0}{k}(\theta - \theta_\infty) + \frac{\sigma\epsilon r_0}{T_0 k}[(\theta T_0 + 273)^4 - (\theta_\infty T_0 + 273)^4] \quad \text{at } R = R_b = r_b/r_0 \tag{18}$$

where

$$A_1 = \frac{v_0 L_t \rho}{\beta_0 g} = \text{Re}$$

= Polymer side Reynolds number

$$A_2 = \frac{3.122 \times 10^{-4} v_0^{0.19} L_t^2}{\beta_0 A_0^{0.905}}$$

$$A_3 = \frac{\rho L_t^2}{\beta_0 v_0} = \frac{\text{Re}}{\text{Fr}}$$

$$\text{Fr} = \text{Froude number} = \frac{v_0^2}{gL_t}$$

$$A_4 = \frac{S_T\sqrt{\pi L_t}}{\beta_0 A_0^{0.5} v_0} = \frac{\text{Re}}{\text{We}}$$

$$\text{We} = \text{Weber number} = \frac{\rho v_0^2 r_0}{gS_T}$$

$$K = \frac{L_t k}{\rho C_p v_0 r_0^2}$$

$$\beta_0 = \beta_\infty \exp\left(\frac{E}{T_0 + 273}\right) \tag{19}$$

NUMERICAL SCHEME

The complicated part of the solutions of Eqs. (10)–(19) lies in the fact that the shape of the fiber and the boundaries r_b and L are not known a priori. Therefore the iterative scheme is necessary. Due to the nonlinearity of the system of equations, the numerical approach becomes essential. In the present analysis a marching finite-difference technique is employed. The steps used for computing the area and temperature profiles are briefly described as follows. Details of numerical analysis can be found elsewhere:[9]

1. In the radial direction of the fiber, r is divided into $M(100)$ equal increments. In the axial direction ΔZ is chosen 0.002865. Since the point N ($L = N\Delta Z$) is unknown, an initial guess is made for N.
2. Guesses on $\eta(Z)$ and $\theta(R, Z)$ are initiated.
3. Φ is calculated from the continuity equation.
4. The finite-difference form of the temperatures in the radial direction is arranged in terms of a tridiagonal matrix and is solved using Gaussian elimination method. Employing a line iterative technique coupling with successive underrelaxation (with a relaxation factor of 0.75–0.8) method, the radial interior temperatures are calculated for a given axial location. The Newton–Raphson method is used to compute the temperature at the boundary.
5. At the Nth node along the axial direction the take-up cross-sectional area Φ is checked. If Φ has not reached the specified exit area, a new value of η is used, which is computed from the shooting method.
6. The computed temperature at the Nth node is checked with the solidified temperature. If they do not agree, the value of N must be increased.
7. With the new values of η and N, steps 3 to 6 are repeated until all boundary conditions are satisfied.

RESULTS AND DISCUSSION

In order to benchmark the present model, we first consider a limiting case with large thermal conductivity and zero emissivity of the fiber. The other parameters employed by Kase and Matsuo[6] are used here:

Take-up diameter, d_t	8 denier
Take-up speed, v_t	500 m/min
Cross-flow air velocity, v_a	20 cm/s
Ambient temperature, T_∞	20°C
Density, ρ	0.83 g/cm^3
Specific heat, C_p	0.70 cal/g °C
Activation energy, E	3500 cal/K
Spinneret diameter d_0	0.4 mm
Spinneret temperature T_0	270°C

These properties represent a low-speed spinning of a polypropylene monofilament. Our numerical results are found to agree well with those of Kase and Matsuo[6] as indicated in Figure 2.

In the present analysis the influence of the following parameters on heat transfer of the polyester fiber are studied. They are dimensionless parameter K, thermal conductivity k, cross-flow velocity v_a, spinneret temperature T_∞, coefficients of inertia, drag, gravity, and surface tension, and the emissivity of the fiber ϵ. Thirty-one different cases are investigated, and the effect of various parameters are examined. The range of aforementioned parameter values are listed in Table I.

In the present computations industrial data on low-speed melt spinning was used. Under this condition the coefficients A_1 to A_4 are negligible.

The dimensionless parameter K characterizes the thermal properties of the polymer, the spinneret properties, and the extrusion velocity. The radial temperature distributions are plotted in Figure 3 for different values of K at axial distance $Z = 0.1433$.

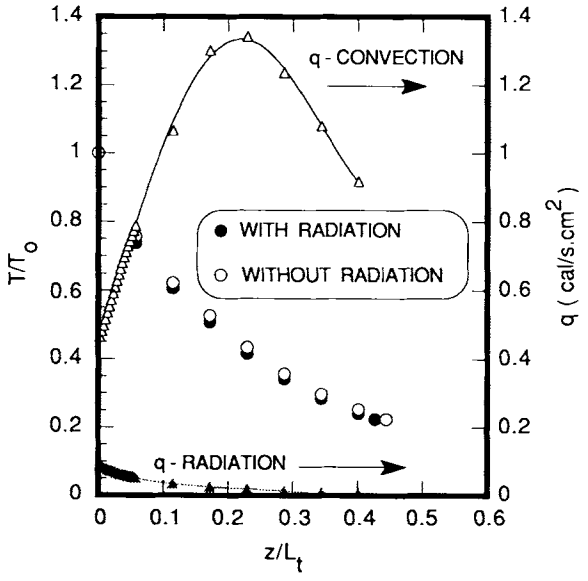

Figure 5 Effect of radiation on melt spinning of a polyester fiber.

To study the effect of K, we set A_1 to A_4 equal to zero. This means η being constant along the axial direction. As the value of K increases, the velocity v_0 is reduced, so that the fiber moves slower. This leads to a higher heat transfer rate, which in turn accelerates the thinning of the fiber. When $K = 7$, the polyester moves relatively faster (as compared with $K = 20$), a longer axial distance is required for fiber to reach its final diameter d_t. Figure 3 reflects that a 7–8°C of temperature difference between the center and surface of the fiber exists. This temperature difference creates an extremely large temperature gradient in radial direction due to a small cross-sectional area of the fiber.

In Figure 4 the variation of cross-sectional area and surface temperature of the fiber with the axial distance is shown. It can be concluded that with the increase in value of K the fiber thins out faster and the final diameter d_t is attained in a shorter axial distance. For example, when $K = 20$, the axial distance is 0.4436 when the surface temperature reaches the solidification temperature (60°C) and fiber attains its final diameter d_t while for $K = 7$ the corresponding required axial distance becomes 1.24. This temperature distribution helps to interpret the internal temperature gradient within the spin line and its effect on the molecular structure of polymers.

Numerical computations reveal a considerable amount of temperature difference between the center and the surface of fiber. Moving away from the spinneret hole, the temperature difference is reduced but is still noticeable for such a small cross-sectional area. These findings imply that the assumption of uniform temperature across the fiber made by the earlier investigators can be misleading.

Another way to estimate the effect of internal resistance of the fiber is to evaluate the Biot number. From *Polymer Handbook*[10] the thermal conductivity of the polyester is approximately 3.3×10^{-4} cal/cm sec °C. The typical heat transfer coefficient lies between 0.3 and 0.8 cal/cm^2 sec °C based on the empirical formula of Kase.[7] Choosing a realistic fiber size (0.025–0.4 mm), we found that the Biot number ($\mathrm{Bi} = hd/k$) is greater than 1.0. The lumped system analysis can only be applied if Bi is less than 0.1. Therefore, neglecting radial heat conduction may give rise to inaccurate results.

Figure 5 shows the temperature ratio distribution for $K = 20$ at different axial positions. The emissivity of the fiber considered here is 0.9. The temperature profiles are evaluated with and without radiation at the boundary. It is evident from this figure that there is significant effect of radiation during the initial period of cooling. Additional insight on the radiation contribution may be observed from Figure 5, which shows the radiative and convective heat fluxes at different axial positions. The contribution of radiation varies from 10 to 15% of the total heat transfer up to 10% of the total axial length.

For different cross-flow velocity the effects of the cross-sectional area of the fiber and surface temperature as function of axial length are shown in Figure 6. As it is expected, increasing the cross-flow air velocity results in faster cooling of the fiber. If the air velocity is increased from 15 to 30 cm/s, the required axial length at which the fiber reaches its final diameter decreases from 0.48 to 0.41. With the increase in cross-flow air velocity the hold up in spinning chamber (L_t) is also reduced.

Figure 7 shows the effects of cooling air temperature, T_∞, on the area of fiber and surface temperature. As expected, the heat transfer rate increases at the lower air temperature, and the axial length required for the fiber to reach the exist diameter decreases. However, the area profile appears to be not very insensitive to the ambient temperature as well as spinneret temperature, T_0 (see Fig. 8). Raising the spinneret temperature will increase the required axial length and also the time required to cool the polyester fiber. These facts are demonstrated in Figure 8. Since the rise in temperature changes the intrinsic viscosity, β, this in turn reduces the fiber tension as well as the force required for drawing the fiber.

To study the effect of coefficients A_1, A_2, A_3, A_4 independently, all other coefficients are set equal to

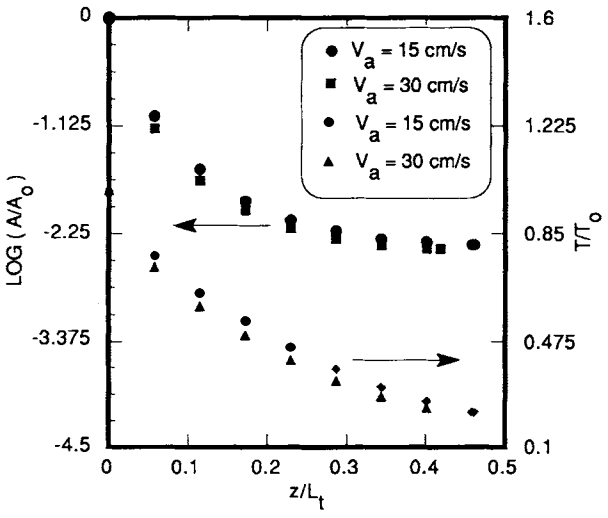

Figure 6 Effect of cross-flow air velocity on area and temperature profiles, L_t = 100 cm, R_0 = 0.02 cm, T_0 = 270°C.

zero except the one under investigation. The temperature and area profiles were computed. Our numerical results reveal that the effects of A_1, A_2, A_3, and A_4 on the surface temperature appear to be relatively small. However, they do affect the cross-sectional area of the polyester fiber. In high-speed melt spinning, inertia and drag are known to have dominant effect. The gravity is important in low-speed spinning of very thick filament, but surface tension is negligibly small in all cases.

CONCLUSIONS

A mathematical model has been developed for studying the dynamics of melt spinning by taking into account radiative heat transfer and radial heat conduction of the fiber, which is subjected to the cooling of cross-flow air. Under a limiting condition of a large conductivity and zero emissivity, the present model is found to agree well with the results of Kase and Matsuo.[6] When a realistic value of conductivity is used, the present results show a significant variation in the radial temperature between the center and the surface of the fiber. The effect of radial temperature variation may have significant effect on polymer crystallization, stress development, and tensile force. The effect of radiation was also studied. It contributes 10–15% of the total heat transfer at the initial stage of cooling of the fiber.

It is found that either increasing the cross-flow air velocity or decreasing the ambient temperature will decrease the polymer hold up in the spin chamber; increasing the spinneret temperature tends to increase the required axial length for fiber to reach the final diameter. It is anticipated that the present results may provide some insight into complicated heat transfer aspects of the polymer processing and may be helpful in developing control strategies in polymer processing.

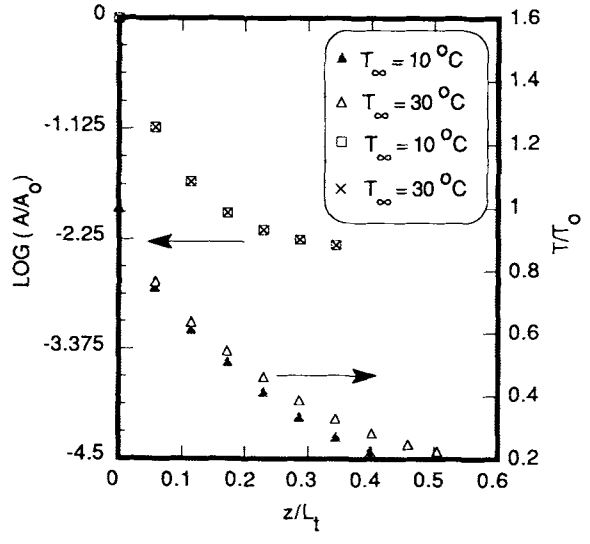

Figure 7 Effect of ambient temperature on area and temperature profiles, L_t = 100 cm, R_0 = 0.02 cm, T_0 = 270°C.

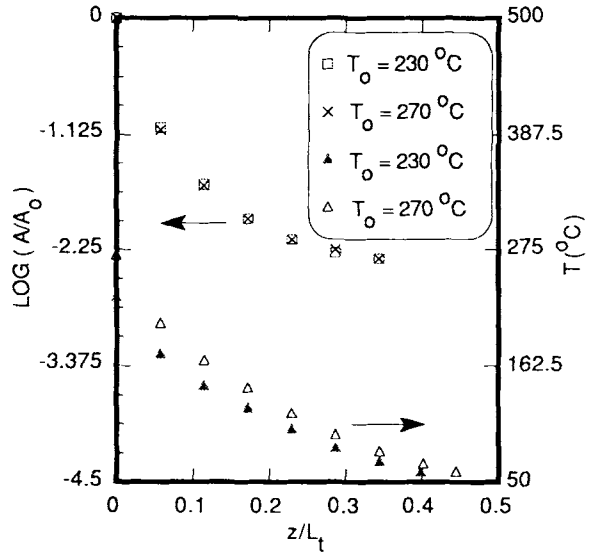

Figure 8 Effect of spinneret temperature on area and temperature profiles, L_t = 100 cm, R_0 = 0.02 cm.

Nomenclature

A	cross-sectional area
A_0	area at the spinneret hole
A_1	inertia coefficient defined by Eq. (19)
A_2	drag force coefficient defined by Eq. (19)
A_3	gravity coefficient defined by Eq. (19)
A_4	surface tension coefficient defined by Eq. (19)
C_p	specific heat
d_0	spinneret hole diameter
d_t	diameter of spun fiber
D_f	drag force
E	activation energy of polymer
F	tensile force
g	gravitational constant
h	heat transfer coefficient
k	thermal conductivity
K	$kL_t/\rho_0(r_0)^2C_pv_0$
L	point where fiber reaches solidification temperature and exit area
L_t	take-up distance
$\dot{m}$	mass flow rate of molten polymer

r	radius of the fiber
r_0	spinneret hole radius
r_b	radius of the fiber at the boundary
R	nondimensional radius
R_0	nondimensional radius at spinneret hole
R_b	nondimensional radius at the boundary
S_T	surface tension
T	temperature
T_s	solidification temperature of polymer
T_0	spinneret temperature
T_∞	ambient temperature
v	velocity
v_a	velocity of cross flowing air
v_0	velocity at the spinneret hole
v_t	take-up velocity
V	nondimensional velocity, v/v_0
V_a	nondimensional cross-flow velocity, v_a/v_0
z	axial direction
Z	nondimensional axial direction, z/L_t
θ	nondimensional temperature, T/T_0
Φ	nondimensional area, A/A_0
η	nondimensional force, $FL_t\{A_0v_0\beta_\infty \exp[E/(T_0 + 273)]\}^{-1}$
θ_∞	nondimensional ambient temperature, T_∞/T_0
ρ	density
ϵ	emissivity
σ	Stefan–Boltzmann constant
β	tensile viscosity
β_∞	material parameter for polymer

References

1. A. Ziabicki, *Fundamental of Fiber Formation,* Wiley, New York, 1986.
2. T. R. Barnett, "Calculation of the Temperature of Filaments in Melt Spinning," *Applied Polymer Symposia,* No. 6, pp. 27–50, 1967.
3. M. Copley and N. H. Chamberlain, "Filament Attenuation in Melt Spinning and Its Effect on Axial Temperature Gradient," *Applied Polymer Symposia,* No. 6, pp. 26–50, 1967.
4. A. Moutsoglou and A. K. Bhattachrya, "Laminar Boundary Layers on Moving Nonisothermal Continuous Cylinders," ASME paper No. 82-HT-74, 1982.
5. M. E. Morrison "Numerical Evaluation of Temperature Profiles and Interface Position in Filaments Undergoing Solidification," *AIChE J.,* **16**(1), 57–63 (1970).
6. S. Kase and T. Matsuo, "Studies on Melt Spinning II Steady State and Transient Solutions of Fundamental Equations Compared with Experimental Results," *J. Appl. Polym. Sci.,* **11,** 251–287 (1967).
7. S. Kase, "Mathematical Simulation of Melt Spinning Dynamics: Steady-State Conditions and Transient Behavior," A. Ziabicki and H. Kawai, Eds., *High Speed Fiber Spinning-Science and Engineering Aspects,* Wiley, New York, 1985.
8. K. Nakamura, K. Katayama, and T. Amano, "Some Aspects of Nonisothermal Crystallization of Polymers. II. Consideration of the Isokinetic Condition," *J. Appl. Polym. Sci.,* **17,** 1031 (1973).
9. V. Iyer, "Heat Transfer from Moving Fibers in Melt Spinning Process," M.S. Thesis, Mechanical Engineering Dept., The University of Akron, Ohio, 1990.
10. E. H. Immergut and J. Brandrup, *Polymer Handbook,* Wiley Interscience, New York, 1975.

Received January 29, 1991
Accepted April 11, 1991